

Effect of temperature change on the behavior of space structures

Lila El-Hefnawy, Fahmy Fath Elbab, and Ahmed Abou- Halawa

Structural Engineering Department, Faculty of Engineering, Alexandria University

Attention to the effect of temperature change on the behavior of space steel structures has been paid. A method for converting the temperature effects into equivalent fictitious joint loads has been presented. A geometrical nonlinear analysis including the effects of axial forces and bowing of space structure members, is used for the analysis and study of the stability of space structures. An algorithm based on the current stiffness parameter is used to predict the buckling behavior of space structures. For this purpose, the tangent stiffness matrix has been used in the analysis, which is carried out by the displacement method through an iterative \ incremental procedure based on Newton-Raphson technique. The iterations that take into account the latest geometry are repeated until the unbalanced loads become negligible and equilibrium is obtained. The equilibrium equations are solved by Cholesky's method. Results of illustrative examples and conclusions based on these results are also given.

تتعرض المنشآت الفراغية الى تغيرات في درجات الحرارة بصورة دورية و هذه التغيرات اما أن تكون مناخية أو ناتجة عن عمليات صناعية مثل المصانع و منشآت التبريد والتجميد أو المنشآت المكيفة الهواء ولذلك فقد تم في هذا البحث دراسة تأثير تغير درجات الحرارة على سلوك و تصرفات المنشآت الفراغية. في هذا البحث تم تحويل تأثير التغيرات الحرارية الى قوى محورية و عزوم انحناء مكافئة تؤثر عند نقاط اتصال المنشآت فقط ليتمكن تحليلها بالطرق العادية للتحليل. كما تم استخدام أسلوب تزايدى تكرارى في التحليل الاخطى مع الأخذ في الاعتبار تأثير القوى المحورية بالأعضاء و الأنحاء و اعتمد أسلوب التحليل أيضا على معامل الكزازة الجارى حيث يمكن باستخدامه يكن اتنبؤ بالسلوك اللاخطى و حمل الانهيار للمنشأ بدقة. أيضا تم عرض طريقة الكزازة كما تم شرح أفضل طرق التقريب المتتالى المستخدمة في الحل و هي طريقة نيوتن. رافسون و الطريقة المعدلة لها. أيضا تم حل معادلات الاتزان بطريقة كلوسكى. كما تم استخدام برنامج للتحليل الاخطى للأخذ في الاعتبار العوامل المذكورة عاليه لدراسة تأثير الحرارة على الحمل الحرج للمنشأ و تصرفه و القوى الداخلية بالأعضاء و الازاحات و الترخيم الحادث بالمنشأ و قد أظهرت نتيجة البحث عن تأثير ملحوظ على سلوك بعض المنشآت الفراغية مثل القباب الهيكلية و الشبكات الفراغية.

Keywords: Nonlinear , Temperature , Space structures , Tangent stiffness matrix , Current stiffness parameter.

1. Introduction

Structures are quite frequently subjected to variations of temperature whose effects are significant that they must be taken into account in the analysis. Such variations may simply be seasonal or may arise as a result of some industrial process such as factories, cooling and freezing building, and air-conditioned building. It is still limited to include the effect of temperature change in the nonlinear analysis and stability of space structures. Temperature changes tend to lead, of course, to changes in the lengths of structure members, if such changes in lengths are completely or partially prevented by conditions at supports or by other parts of the structure then stresses will be set up in some or all of the members. So recommendations have been made for the

inclusion of the effects of temperature in the nonlinear analysis of space structures.

The present investigation presents a nonlinear analysis of three-dimensional skeletal steel structures considering the effects of temperature changes. The analysis includes the effects of axial forces and bowing of space frame members, by using stability functions and bowing functions and by using the tangent stiffness matrix of space frame members derived on the basis of deformed geometry of the members. A geometrical nonlinear incremental/iterative technique is used for the analysis and study of the stability of space structures. An algorithm based on the current stiffness parameter S_p is implemented in the study to predict the buckling behavior of space structures. The current stiffness parameter has also been used for the automation of the load incrementation procedure and for detecting and

parameter has also been used for the automation of the load incrementation procedure and for detecting and determining the existence and the type of such instabilities as might arise during load application.

Temperature effects are converted into equivalent joint loads and are treated as a temperature loading condition. The deformations due to temperature are superposed on the deformations caused by live load.

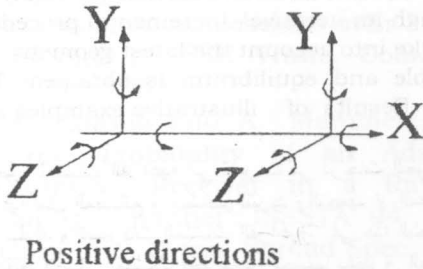


Fig. 1. Member axes in undeformed geometry and sign convention for forces and displacements.

2. Sign convention

The joint translations and forces acting on the member are positive along the positive directions of the coordinate axes, while the positive directions of the joint rotations and moments are determined in accordance with the right hand screw rule fig. 1. For convenience, both the translations and rotations will be referred to as deformations and, similarly, direct forces and moments will be termed joint loads.

3. Coordinate axes systems

The forces and deformations at the ends of a structural element are usually referred to as individual set of right handed axes. When the relative end deformations and the independent end forces are considered, these axes will be referred to as the member or local current axes (x^c, y^c and z^c) The equilibrium check equations (i.e the nonlinear relations between the relative end deformations and the independent

components of the end forces) have been derived throughout this research with respect to these local current axes. A further set of local axes has also been used, and this will be referred to as the member or local updated axes x, y and z , fig. 2.

In such member local updated axes, the relations between all element end forces(including the dependent component) and end deformations are derived with respect to the element updated axes allowing for the latest known geometry of the structure. In both the x^c, y^c, z^c and the x, y, z systems, the member centroidal axis is taken as the x axis, while the major and minor principal bending axes y and z are a moving coordinate system. Also the principal directions of bending (the direction of the y and z axes) will vary for deformed members from one cross section to another. The y and z axes defined herein therefore, refer to an average cross-section.

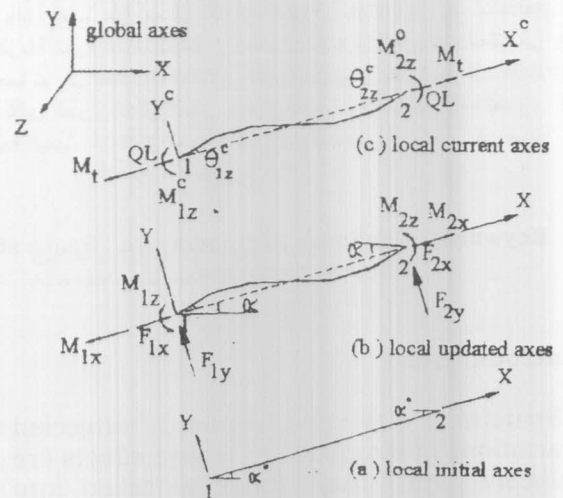


Fig. 2. Systems of coordinate axes.

On the other hand, in order to write the equilibrium equations of the complete system, all the joint deformations and loads for the structure are expressed in a single fixed global coordinate system X, Y and Z . These will be referred to as structure or global axes.

4. Stiffness matrices of standered members

The equilibrium check equations which include the effects of axial force and bowing can be written in the form

$$\begin{aligned} M^{c_{1z}} &= EI_z(c_{1z}\theta^{c_{1z}} + c_{2z}\theta^{c_{2z}}) / L, \\ M^{c_{2z}} &= EI_z(c_{2z}\theta^{c_{1z}} + c_{1z}\theta^{c_{2z}}) / L, \\ M^{c_{1y}} &= EI_y(c_{1y}\theta^{c_{1y}} + c_{2y}\theta^{c_{2y}}) / L, \\ M^{c_{2y}} &= EI_y(c_{2y}\theta^{c_{1y}} + c_{1y}\theta^{c_{2y}}) / L, \\ M_t &= GJ\omega_t / L, \\ Q &= EA(u - \delta_{by} - \delta_{bz}) / L, \end{aligned} \tag{1}$$

where $c_{1z}, c_{2z}, c_{1y}, c_{2y}$ are the stability functions and δ_{by}, δ_{bz} are the axial shortening due to bowing about axes y^c, z^c

The level of the axial force Q can be related to Euler load through a non-dimensional axial force parameter q thus

$$\begin{aligned} q &= Q / P_{Euler} \\ &= (EA/L)(u - \delta_{by} - \delta_{bz}) / (\pi^2 EI / L^2) \\ &= (s^2 / \pi^2)(\mu - c_{by} - c_{bz}), \end{aligned} \tag{2}$$

where:

- s is the slenderness ratio $= L / (I/A)^{1/2}$
- μ is the total axial strain u/L
 $u = u_{x1} - u_{x2}$
- c_{by}, c_{bz} are the axial strain due to bowing about the principal axes
- I is the reference moment of inertia
 $\omega_t = \theta^{c_{x1}} - \theta^{c_{x2}}$

The expression for the axial force Q in Eq.(1) can be written in terms of the non-dimensional axial force parameter

$$QL = (EI/L)(q\pi^2). \tag{3}$$

The equilibrium check equation derived above for a space frame member, will be used to establish the member tangent stiffness matrix in the global axes (X,Y,Z) (K_t). To achieve this, the member tangent stiffness matrix will be first established for relative deformations in the member local current axes x^c, y^c and z^c . The second step will be the transformation of this tangent stiffness matrix [t] into its local updated axes x, y and z to obtain [T]. The third step will be

the transformation of [T] To the structure global axes to obtain $[k_t]$. The development presented in this section generally follows that of Oran(1).

4.1. The tangent stiffness matrix in the member local axes(x^c, y^c, z^c)

The expressions in Eq.(1) can be written in the form

$$\{S\} = \{f(u)\}, \tag{4}$$

where $\{S\}$ is the vector of the nodal forces, (u) are the nodal deformations, and f are a set of nonlinear functions in u which include the effects of axial force, and bowing.

For any given displacement u , Eq.(4) can be differentiated to give

$$\{\Delta S\} = [t]\{\Delta u\}, \tag{5}$$

where

$$\begin{aligned} \{\Delta S\}^T &= \{\Delta M^{c_{1z}}, \Delta M^{c_{2z}}, \Delta M^{c_{1y}}, \Delta M^{c_{2y}}, \Delta M_t, \Delta QL\}, \\ \{\Delta u\}^T &= \{\Delta \theta^{c_{1z}}, \Delta \theta^{c_{2z}}, \Delta \theta^{c_{1y}}, \Delta \theta^{c_{2y}}, \Delta \omega_t, \Delta \mu\}, \end{aligned} \tag{6}$$

and $[t]$ is the tangent stiffness matrix for relative displacements. The element t_{ij} of $[t]$ is

$$t_{ij} = \partial S_i / \partial u_j = \partial S_i / \partial \theta_j \quad \text{for } j=1,2,3,4,5,6 \tag{7}$$

Taking into consideration the following Oran [9] relations

$$\frac{\partial q}{\partial \theta^{c_{mn}}} = \frac{G_{mn}}{\pi^2 H}, \quad \frac{\partial q}{\partial \omega_t} = 0, \quad \frac{\partial q}{\partial u} = \frac{1}{H}, \tag{8}$$

where:

$$\begin{aligned} G_{1n} &= c / {}_{1n}\theta^{c_{1n}} + c / {}_{2n}\theta^{c_{2n}}, \\ G_{2n} &= c / {}_{2n}\theta^{c_{1n}} + c / {}_{1n}\theta^{c_{2n}}, \\ H &= (\pi/s)^2 + \sum_{n=y,z} [b / {}_{1n}(\theta^{c_{1n}} + \theta^{c_{2n}})^2 + b / {}_{2n}(\theta^{c_{1n}} + \theta^{c_{2n}})^2], \end{aligned}$$

in which the subscript m refers to the member ends 1 or 2, the subscript n refers to the axes y^c, x^c and the prime superscript indicates one differentiation with respect to q_n . Using expressions in Eqs. (1),(2),(3) and performing the differentiation in Eq.(7) lead to the member

tangent stiffness matrix [t] in the local current axes (x^c, y^c, z^c) .

$$[t] = EI/L \times [t_{ij}] \tag{9}$$

where:

$$\begin{aligned} t_{1.1} &= \zeta_z C_{1z} + G_{1z}^2 / (\pi^2 H), \\ t_{1.2} &= \zeta_z C_{2z} + (G_{1z} G_{2z}) / (\pi^2 H), \\ t_{1.3} &= 0, \\ t_{1.4} &= 0, \\ t_{1.5} &= 0, \\ t_{1.6} &= G_{2z} / H, \\ t_{2.1} &= \zeta_z C_{2z} + (G_{1z} G_{2z}) / \pi^2 H, \\ t_{2.2} &= \zeta_z C_{1z} + G_{2z}^2 / (\pi^2 H), \\ t_{2.3} &= 0, \\ t_{2.4} &= 0, \\ t_{2.5} &= 0, \\ t_{2.6} &= G_{2z} / H, \\ t_{3.1} &= 0, \\ t_{3.2} &= 0, \\ t_{3.3} &= \zeta_y C_{1y} + G_{1y}^2 / (\pi^2 H), \\ t_{3.4} &= \zeta_y C_{2y} + G_{1y} G_{2y} / (\pi^2 H), \\ t_{3.5} &= 0, \\ t_{3.6} &= G_{1y} / H, \\ t_{4.1} &= 0, \\ t_{4.2} &= 0, \\ t_{4.3} &= \zeta_y C_{2y} + G_{1y} G_{2y} / (\pi^2 H), \\ t_{4.4} &= \zeta_y C_{1y} + G_{2y}^2 / (\pi^2 H), \\ t_{4.5} &= 0, \\ t_{4.6} &= G_{2y} / H, \\ t_{5.1} &= 0, \\ t_{5.2} &= 0, \\ t_{5.3} &= 0, \\ t_{5.4} &= 0, \\ t_{5.5} &= \eta_t, \\ t_{6.1} &= G_{1z} / H, \\ t_{6.2} &= G_{2z} / H, \\ t_{6.3} &= G_{1y} / H, \\ t_{6.4} &= G_{2y} / H, \\ t_{6.5} &= 0, \\ t_{6.6} &= \pi^2 / H, \end{aligned}$$

where $\eta_t = GJ/EI$, $\zeta_z = I_z/I$, $\zeta_y = I_y/I$,

4.2. The tangent stiffness matrix in the member local updated axes (x, y, z)

If {F} denotes a 12x1 vector representing member end forces referred to the member local updated axes (x, y, z) these forces can be related to the member end forces in the local

current axes (x^c, y^c, z^c) by the equilibrium equations to give

$$\{F\} = [B^1] \{S\}, \tag{10}$$

in which [B] is the local static or equilibrium matrix

$$[B] = \begin{pmatrix} 0 & 0 & 0 & 0 & 0 & 1/L \\ 1/L & 1/L & 0 & 0 & 0 & 0 \\ 0 & 0 & -1/L & -1/L & 0 & 0 \\ 0 & 0 & 0 & 0 & -1 & 0 \\ 0 & 0 & 1 & 0 & 0 & 0 \\ 1 & 0 & 0 & 0 & 0 & 0 \\ 0 & 0 & 0 & 0 & 0 & -1/L \\ -1/L & -1/L & 0 & 0 & 0 & 0 \\ 0 & 0 & 1/L & 1/L & 0 & 0 \\ 0 & 0 & 0 & 0 & 1 & 0 \\ 0 & 0 & 0 & 1 & 0 & 0 \\ 0 & 1 & 0 & 0 & 0 & 0 \end{pmatrix}$$

and

$$\{F\}^T = \{F_{1x}, F_{1y}, F_{1z}, M_{1x}, M_{1y}, M_{1z}, F_{2x}, F_{2y}, F_{2z}, M_{2x}, M_{2y}, M_{2z}\}, \tag{11}$$

$$[T] = [B][t][B]^T, \tag{12}$$

where [T] is the 12x12 element local stiffness matrix which relates the end forces to the corresponding end deformations in the directions of the member local coordinates (x, y, z)

4.3. The overall stiffness matrix in the structure global axes (X, Y, Z)

To construct the overall structure tangent stiffness matrix, the individual element tangent stiffness matrices should be transferred from their local updated coordinates (x, y, z) to the structure global coordinates (X, Y, Z) . Let [R] be a 12x12 orthogonal matrix defined by

$$[R] = \begin{pmatrix} [r_1] & 0 & 0 & 0 \\ 0 & [r_1] & 0 & 0 \\ 0 & 0 & [r_2] & 0 \\ 0 & 0 & 0 & [r_2] \end{pmatrix} \tag{13}$$

in which $[r_1], [r_2]$ are the end section orientation matrices defined by the member

orientation matrix $[r]$ and the orientation matrices of joints 1 and 2 $[\alpha_1], [\alpha_2]$, respectively.

Note that $[r]$ depends on the direction cosines of the member local updated axes (x,y,z) with respect to the structure global axes (X,Y,Z) and $[\alpha_1], [\alpha_2]$ depend on the individual rotations of each end of the member.

If $[k_i]$ is the member tangent stiffness matrix in the structure global axes

$$[k_i] = [R][T][R]^T \quad (14)$$

$$= [R][B][t][B]^T[R]^T \quad (15)$$

$$= [B][t][B]^T \quad (16)$$

in which $[B]$ is the instantaneous global equilibrium matrix

$$[B] = [R][B] \quad (17)$$

The overall stiffness matrix is

$$[K_T] = \Sigma [B][t][B]^T \quad (18)$$

5. Nonlinear analysis and stability

5.1. Method of solution

The method of solution is based on the principles of potential energy or virtual work. A balance equation between the applied external forces $\{P\}$ and the integrated internal forces $\{P^{int}\}$ is sought in the displaced state

$$\{P\} = \{p^{int}\} \quad (19)$$

Often the applied forces $\{P\}$, which at equilibrium are equal to internal forces $\{p^{int}\}$, are expressed by

$$\{P\} = \{p^{int}\} = [K_s]\{v\} \quad (20)$$

where $[K_s]$ is often denoted either as "The secant stiffness matrix" or the "equilibrium check" equations

The next level of equations can be obtained by using the differential form of the equilibrium check equations

$$\{P'\} = [K_i]\{v'\} \quad (21)$$

where dash denotes differentiation with respect to a loading parameter λ . Eq.(21) can be also be written in incremental form as

$$\{\Delta P\} = [K_i]\{\Delta v\} \quad (22)$$

By substituting for $[K_i]$ the tangent stiffness matrix $\{K_T\}$, Eq. (22) at station i in the iteration sequence can be written in the form

$$\{\Delta P\}_{i+1} = [K_T]_i \{\Delta v\}_{i+1} \quad (23)$$

5.2. Incremental and iterative schemes

Consider load level $\{P_i\}$, and assume that the corresponding deformation configuration of the system $\{v_i\}$ is known. It is now desired to determine the configuration $\{v_{i+1}\}$ corresponding to load level $\{P_{i+1}\}$ where

$$\{P_{i+1}\} = \{P_i\} + \{\Delta P_{i+1}\} \quad (24)$$

In the following discussion, subscript "j" is used to refer to the j^{th} iteration cycle within load increment i . The out of balance force for iteration j is

$$\{P_{i,j}^{ob}\} = \{P_{i+1}\} - \{P_{i,j}^{int}\} \quad (25)$$

in which $\{P_{i+1}\}$ is the level of the external applied load, and $\{P_{i,j}^{int}\}$ represents the internal joint forces corresponding to the configuration $\{v_{i,j}\}$. The out of balance joint forces are then treated as a load increment and the displacement correction vector $\{\Delta v_{i,j}\}$ is obtained from the incremental relationship

$$[K_{T,j}]\{\Delta v_{i,j+1}\} = \{P_{i,j}^{ob}\} \quad (26)$$

and a new approximate configuration can be obtained from the equation

$$\{v_{i,j+1}\} = \{v_{i,j}\} + \{\Delta v_{i,j+1}\} \quad (27)$$

The process continues until the prescribed tolerance of the convergence criteria is achieved.

5.3. Updating the deformation

The current node positions can be found by adding the transitional components of the current displacement vector $\{v_{i+1}\}$ to the coordinates of the joints at the previous load level

$$\{v_{i+1}\} = \{v_i\} + \{\Delta v_{i+1}\} \quad (28)$$

To update the nodal orientation and the shape of members the rotational components of the displacement vector should be updated.

For small incremental rotation components an approximate value for the current rotations can be obtained as before using Eq.(28). However, for large values of the incremental rotational components the method presented by Oran is used in this paper.

5.4. Computation of member relative deformation and orientation

The orientation of the member updated axes (x,y,z) with respect to the global structure axes (X,Y,Z) is best described by the orthogonal direction cosine matrix $\{r\}$

$$[r] = \begin{bmatrix} \cos Xx & \cos Xy & \cos Xz \\ \cos Yx & \cos Yy & \cos Yz \\ \cos Zx & \cos Zy & \cos Zz \end{bmatrix}$$

$$= \begin{bmatrix} L_x & -L_x L_y \cos \gamma - L L_z \sin \gamma & L_x L_y \sin \gamma - L L_z \cos \gamma \\ L & L(L^2_x + L^2_z)^{1/2} & L(L^2_x + L^2_z)^{1/2} \\ L_y & (L^2_x + L^2_z)^{1/2} \cos \gamma & -(L^2_x + L^2_z)^{1/2} \sin \gamma \\ L & L & L \\ L_z & -L_y L_z \cos \gamma + L L_x \sin \gamma & L_y L_z \sin \gamma - L L_x \cos \gamma \\ L & L(L^2_x + L^2_z)^{1/2} & L(L^2_x + L^2_z)^{1/2} \end{bmatrix}$$

where

$$L_x = X_2 - X_1, \quad L_y = Y_2 - Y_1, \quad L_z = Z_2 - Z_1$$

$$L = \sqrt{L_x^2 + L_y^2 + L_z^2}, \quad (29)$$

and γ is the orientation angle between the xy and x_0y_0 planes where y_0 is a special vertical axes parallel to the global Y axes, and x_0 coincides with the member current x axes at the initial un-deformed state of the member

It is worth noting that the derivation of the rotation matrix in Eq.(29) for the initial position of a member, involves three rotation matrix $[r_0^\alpha], [r_0^\beta]$ and $[r_0^\gamma]$ and the multiplication of these three matrices results in the final initial member rotation matrix $[r_0]$

$$[r_0] = [r_0^\gamma][r_0^\beta][r_0^\alpha]. \quad (30)$$

For small relative twisting of the ends, the average twist γ_i^{ave} at deformed position i may be related to the orientation angle γ_0 at the initial un-deformed position by

$$\gamma_i^{ave} \approx \gamma + (\theta_{1x} + \theta_{2x}) / 2, \quad (31)$$

in which

$$\begin{aligned} \theta_{1x} &\approx (L_x/L)\theta_{1x} + (L_y/L)\theta_{1y} + (L_z/L)\theta_{1z} \\ \theta_{2x} &\approx (L_x/L)\theta_{2x} + (L_y/L)\theta_{2y} + (L_z/L)\theta_{2z} \end{aligned} \quad (32)$$

For a deformed member, let X_1, Y_1, Z_1 and X_2, Y_2, Z_2 be its joint co-ordinates and $[\alpha_1], [\alpha_2]$ the associated joint orientation matrices of its two joints. Due to the fact that the two end sections of the member will not be exactly paralleled to each other, let $[\rho_1], [\rho_2]$ be "the end section orientation matrices" where these matrices represent the combined effect of both the joint orientation matrix and the member orientation matrix. It then follows that

$$\begin{aligned} [\rho_1] &= [\alpha_1][r_0], \\ [\rho_2] &= [\alpha_2][r_0], \end{aligned} \quad (33)$$

where $[r_0]$ is the member orientation matrix in the initial un-deformed configuration. To define the current member orientation matrix, $[r]$, the first column of the matrix $\{r_{11}, r_{21}, r_{31}\}^T$, as well as the relative axial displacements μ , can be obtained from the member end coordinates $\{x_1, y_1, z_1\}^T$ and $\{x_2, y_2, z_2\}^T$. Also due to the small relative

deformation assumption adopted in normal beam column theory, the relative end rotation angles in the member current axes $\{\theta^{c_{1y}}, \theta^{c_{1z}}, \theta^{c_{2y}}, \theta^{c_{2z}}\}^T$ can be obtained as scalar products of the first column $\{r^{(1)}\}$ of the current member orientation matrix with appropriate column of $[\rho_1], [\rho_2]$, thus

$$\begin{aligned} [\rho_1]^T \{r^{(1)}\} &\approx \{1 - \theta^{c_{1z}} \quad \theta^{c_{1y}}\}^T \text{ to get } \theta^{c_{1z}}, \theta^{c_{1y}}, \\ [\rho_2]^T \{r^{(1)}\} &\approx \{1 - \theta^{c_{2z}} \quad \theta^{c_{2y}}\}^T \text{ to get } \theta^{c_{2z}}, \theta^{c_{2y}}, \\ \text{similarly} \\ \omega_i &\approx -\{\rho_1^{(2)}\}^T \{\rho_2^{(3)}\} \approx \{\rho_1^{(3)}\}^T \{\rho_2^{(2)}\}, \end{aligned} \tag{34}$$

where ω_i is the relative twist between the ends. The subscripts (1), (2) and (3) indicates the column number of the matrices used.

To determine the second and third columns of $[r]$, let $\{e_1\}, \{e_2\}$ be the joint orientation matrices in the local current axes after rotating the end sections about their principal directions y^c, z^c but not about their normal axis x , in such a way as to make these sections perpendicular to the member x -axis (i.e. $\omega_i = 0.0$) thus

$$\begin{aligned} \{e_1\} &= \begin{bmatrix} 1 & \theta^{c_{1z}} & -\theta^{c_{1y}} \\ -\theta^{c_{1z}} & 1 & 0 \\ \theta^{c_{2y}} & 0 & 1 \end{bmatrix} \text{ and} \\ \{e_2\} &= \begin{bmatrix} 1 & \theta^{c_{1z}} & -\theta^{c_{2y}} \\ -\theta^{c_{2x}} & 1 & 0 \\ \theta^{c_{2y}} & 0 & 1 \end{bmatrix}. \end{aligned} \tag{35}$$

In this situation, the new end section orientation matrices will be given by

$$\begin{aligned} [r_1] &\approx [\rho_1][e_1], \text{ and} \\ [r_2] &\approx [\rho_2][e_2] \end{aligned} \tag{36}$$

For small relative rotation ω_i the member orientation matrix $[r]$ of an average cross section will be taken as the average of the end section orientation matrices $[r_1], [r_2]$, thus

$$[r] \approx \frac{1}{2} [[r_1] + [r_2]] \tag{37}$$

5.5. Current stiffness parameter S_p

To formulate the value of S_p , consider a structure in a converged equilibrium state under a certain level of load $\{P_{i-1}\}$ and consider an increment of load $\{\Delta P_i\}$ and the corresponding increment in the displacement vector of $\{\Delta v_i\}$. For proportional loading the load $\{p_i\}$ at level i can be expressed in terms of a reference load $\{p_{ref}\}$ through a scalar load parameter λ_i , thus ref. [2,5].

$$\{p_{i-1}\} = \lambda_{i-1} \{P_{ref}\}. \tag{38}$$

The subsequent load increment at stage i can also be expressed by this scalar load parameter,

$$\{\Delta P_i\} = \lambda_{i-1} \{P_{ref}\}. \tag{39}$$

So the current stiffness parameter of the structure can then be expressed as

$$\frac{d\lambda_i L}{dv_i} = \frac{\Delta\lambda_i L}{\Delta v_i} = \frac{1}{v_i'} \tag{40}$$

where v_i' is then the differential of v_i with respect to λ_{i-1} . Expression (40) for the current stiffness is a vector. It can be transformed into a scalar through multiplication by the reference load vector $\{P_{ref}\}$.

$$\begin{aligned} \text{The scalar current stiffness} &= \frac{1}{\{v_i'\}^T \{P_{ref}\}} \\ &= \frac{\Delta\lambda_{i-1}}{\{v_i'\}^T \{P_{ref}\}}. \end{aligned} \tag{41}$$

The initial stiffness, which is the stiffness corresponding to the first load increment ΔP_1 can be expressed in a similar fashion as

$$\begin{aligned} \text{The initial stiffness} &= (d\lambda_{i-1}/dv)_1 = 1/\{v_1'\} \\ &= \Delta\lambda_{i-1}/\{\Delta v_1\} \end{aligned} \tag{42}$$

The subscript 1 in Eq. (42) indicates the first load increment starting from the initial state.

The scalar current stiffness for increment i can now be related to the initial scalar stiffness at increment 1 i.e. Eq. (42) modified in the

same way as the current stiffness in Eq.(43) to give

$$S_p = \frac{\text{The scalar current stiffness}}{\text{The scalar initial stiffness}}$$

$$= \frac{\Delta\lambda_i L}{\{\Delta v_i\}^T \{P_{ref}\}} / \frac{\Delta\lambda_{i1} L}{\{\Delta v_i\}^T \{P_{ref}\}}, \quad (43)$$

$$= \frac{\Delta\lambda_i L \{\Delta v_i\}^T \{P_{ref}\}}{\Delta\lambda_{i1} L \{\Delta v_i\}^T \{P_{ref}\}}.$$

S_p is defined as "the current stiffness parameter" when $\{\Delta v_i\}$ is calculated using the current tangent stiffness matrix

$$\{\Delta P_i\} = [K_T]_i \{\Delta v_i\}. \quad (44)$$

By substituting the value of $\{P_{ref}\}$ from Eq.(38) in Eq. (42) an alternative expression for S_p can be obtained as

$$S_p = \frac{(\Delta\lambda_i L)^2 \{\Delta v_i\}^T \{\Delta P_i\}}{(\Delta\lambda_{i1} L)^2 \{\Delta v_i\}^T \{\Delta P_i\}}. \quad (45)$$

Which with the values of $\{\Delta P_i\}$ and $\{P_{ref}\}$ from Eqn.(44) gives

$$S_p = (\Delta\lambda_i L / \Delta\lambda_{i1} L)^2 (D_1 / D_i), \quad (46)$$

where D_1 and D_i are scalar values given by

$$D_1 = \{\Delta v_i\}^T [K_T]_1 \{\Delta v_i\},$$

$$D_i = \{\Delta v_i\}^T [K_T]_i \{\Delta v_i\},$$

where $[K_T]_1, [K_T]_i$ are the tangent stiffness matrices at the initial and current states of equilibrium.

6. Equivalent temperature end forces

Figure 3 shows a member of length L subjected to a temperature rise ΔT which is uniform throughout its volume. If the bar is free to expand its length will increase by

$$e = \alpha \cdot \Delta T \cdot L$$

If the expansion is prevented completely a compressive axial force will be set up in the member. This force has a magnitude of

$$F = AEe/L$$

$$F = \alpha \cdot E \cdot A \cdot \Delta T. \quad (47)$$

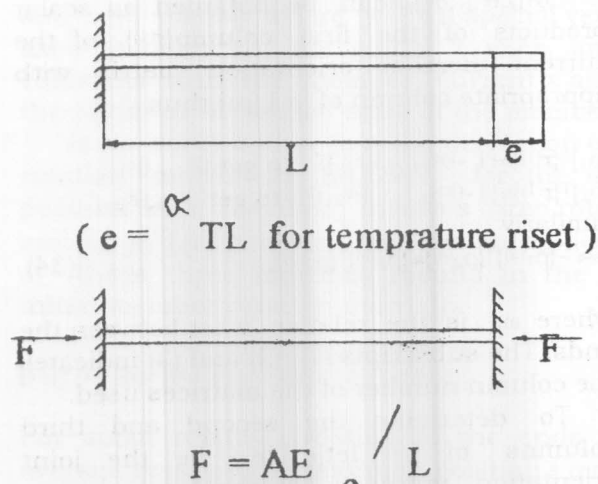


Fig. 3. The fixed end forces due to temperature change.

In the above equation, only the simplest kind of temperature change effect has been considered which is the change of length of the element. This leads to fixed-end forces acting in the axial direction. Other situations may result in different types of fixed-end-forces. Some of these situations which will lead to the occurrence of fixed-end-moments will now be considered.

In problems of temperature changes it is quite common for one or more elements of a structure to be subjected to a thermal gradient rather than to a uniform temperature change. Such a situation is shown in Fig. 4. The manner of variation of the temperature through the depth and width is linear.

There will in general be changing in length of the centroidal axes plus rotations. The latter takes place as a result of the difference in thermal strain through the beam depth and width. The changing in length behavior will be prevented by fixed-end axial forces of the type described before, which have magnitude $\alpha \cdot A \cdot E \cdot \Delta T$. It should be noted that ΔT is the temperature change at the centroid.

$$\Delta T = \Delta T_1 + \Delta T_2 + \Delta T_3 + \Delta T_4 \quad (48)$$

The bending behavior is the same at all points along the beam and therefore the beam will bend in a circular arc. The strain at the top or the bottom edge is algebraically added to the centroidal strain, using the simple bending formula.

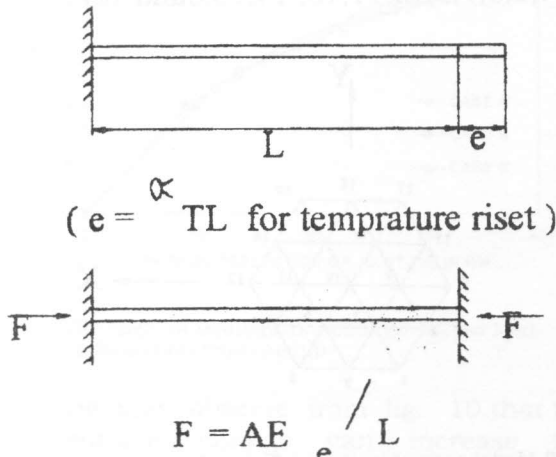


Fig.4. The fixed end- moments due to temperature Change.

The fixed-end moment which would be required to prevent the bending deformation has the magnitude

$$M_z = EI_z \alpha (\Delta T_1 - \Delta T_2) / d, \quad (49)$$

$$M_y = EI_y \alpha (\Delta T_3 - \Delta T_4) / b, \quad (50)$$

where d,b are the depth and the width of the cr cross-section of the member respectively.

7. Numerical examples

Example 1

The space frame shown in figure 5 has been analyzed under uniform temperature change. All members have the same cross-section with following properties:

$$\begin{aligned} A &= 1385.44 \text{ mm}^2 & I_y = I_z &= 695838.43 \text{ mm}^4 \\ J &= 1391676.85 \text{ mm}^4 & E &= 210 \text{ KN/mm}^2 \\ G &= 81 \text{ KN/mm}^2 & \alpha &= 11 \times 10^{-6} \end{aligned}$$

The frame is carrying a vertical concentrated live load at joint 1.

Figure 6 shows the load-deformation relationship of joint 1 for the following three cases.

Case A Live load only.

Case B Live load + uniform temperature rise = 40°C.

Case C Live load + uniform temperature drop = -40°C.

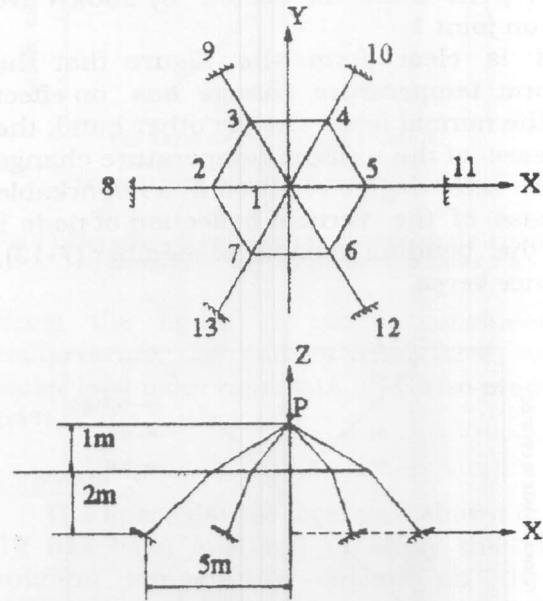


Fig.5. Model geometry and node numbers of space frame

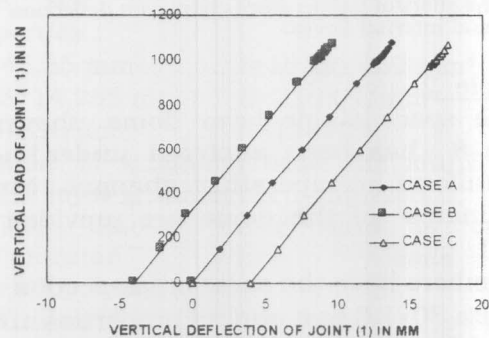


Fig. 6. The effect of temperature change on the load-deformation relationship.

It is clear from the figure that except some deformation there is no other effects on the load-deformation relationship. The maximum loads in three cases are approximately the same. This means that it is possible for such type of structures to be subjected to

temperature change and yet remain unstressed.

Figure 7 shows the effect of uniform temperature change on the vertical displacement of joint 1, normal force in member (7-13) and M_z of member (7-13) at end (7). The frame is loaded by 200KN live load on joint 1.

It is clear from the figure that the uniform temperature change has no effect on the normal force. On the other hand, the decrease of the uniform temperature change below zero degree resulted in a remarkable increase of the vertical deflection of node 1 and the bending moment of member (7-13), and vice versa.

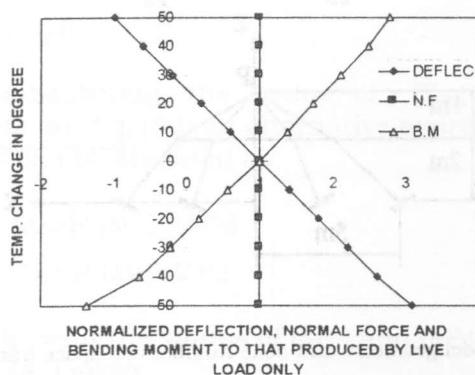


Fig. 7. The effect of temperature change on deflection and internal forces.

Example 2

The space single layer dome shown in Figure 8 has been analyzed under linear and uniform temperature changes. Nodal co-ordinates of the dome are provided in Table.1.

All members have the same cross-section tube size 30x1.6 mm and its properties are:

- A=143.35mm² I=15156.069mm⁴
- J=28714.285mm⁴ E=210KN/mm²
- G=81KN/mm² $\alpha=11 \times 10^{-6}$

The six support nodes (1,3,8,12,17and19) are totally fixed. The dome is carrying live loads at nodes (2,4,5,7,9,10,11,13,14,15,16and 18).

Figure 9 shows the effect of linear temperature change on the load-deformation relationship for the following three cases:

Case A Live load only

Case B Live load + linear temperature change ($\Delta T_{in}=-20^{\circ}C$ & $\Delta T_{out}=+20^{\circ}C$)

Figure 10 shows the effect of uniform temperature change on the vertical deflection of joint (10) , normal force in member (6-10) and M_z of member (6-10) at end (6) relative to that produced by 0.1 KN live load on nodes (2,4,5,6,7,9,10,11,13, 14,15,6and 18) .

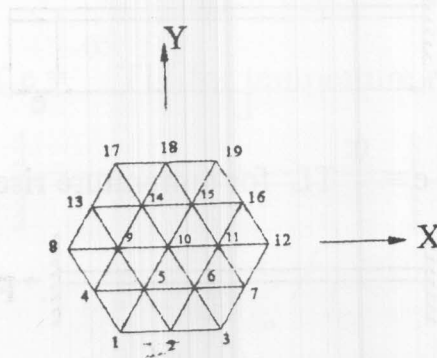


Fig.8.Model geometry and node numbers .

Table. 1 Nodal co-ordinate of space single layer dome

	X mm	Y mm	Z mm
1	-2500.0	-4330.1	0.00
2	0.00	-4330.1	100.5
3	2500.0	-4330.1	0.00
4	-3750.0	-2165.1	100.5
5	-1250.0	-2165.1	300.5
6	1250.0	-2165.1	300.5
7	3750.0	-2165.1	100.5
8	-5000.0	0.00	0.00
9	-2500.0	0.00	300.5
10	0.00	0.00	400.0
11	2500.0	0.00	300.5
12	5000.0	0.00	0.00
13	-3750.0	2165.1	100.5
14	-1250.0	2165.1	300.5
15	1250.0	2165.1	300.5
16	3750.0	2165.1	100.5
17	-2500.0	4330.1	0.00
18	0.00	4330.1	100.5
19	2500.0	4330.1	0.00

Case C Live load + linear temperature change ($\Delta T_{in}=+20^{\circ}C$ & $\Delta T_{out}=-20^{\circ}C$)

It can be noticed from fig. 9 that either case B or case C decreases the maximum carried load by about 20%.

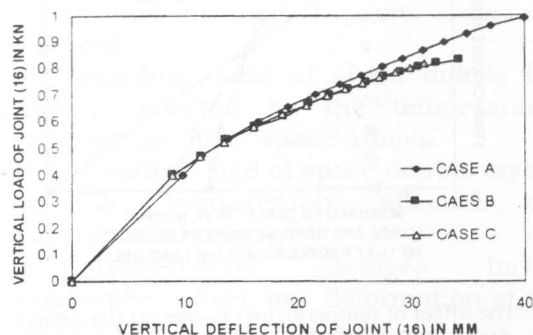


Fig. 9 The effect of temperature change on the load-deformation relationship.

One may observe from fig. 10 that the temperature change can increase the deflection, normal force and bending moment many times or reverse them to the opposite directions. Also, excessive temperature drop makes the stresses in some members reach yielding stress without any increase in live load.

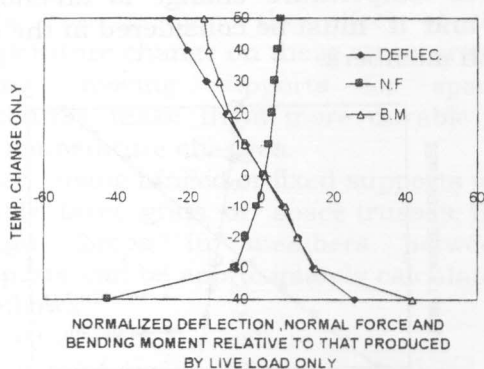


Fig. 10. The effect of temperature change on the deflection and internal forces.

Figure 11 shows the ratio of the normal force in member (6-10) resulting from temperature change only compared with Euler load.

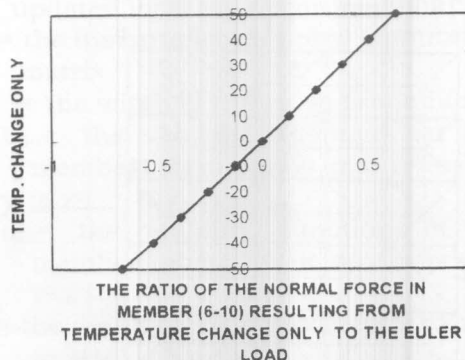


Fig. 11 The effect of temperature change on the normal force in member (6-10) compared with Euler load.

From the figure it can be concluded that temperature rise causes axial force to reach Euler load more rapidly. (A 50°C rise produces \approx 64% of the Euler load.)

Example 3

The space double layer grid shown in figure 12 has been analyzed to study the effect of uniform temperature change on the load-deformation relationship, the maximum load carrying capacity, deformations, and internal forces.

All members have the same cross-section: a tube size 30x1.6 mm with the following properties:

$$A=143.35 \text{ mm}^2 \quad I=15156.069 \text{ mm}^4$$

$$J=28714.285 \text{ mm}^4 \quad E=210 \text{ KN/mm}^2$$

$$G=81 \text{ KN/mm}^2 \quad \alpha=11 \times 10^{-6}$$

Because of symmetry only one fourth of the double layer grid has been analyzed.

The double layer grid is carrying concentrated live loads at nodes (5,6,7,12,13,14, 19,21, and 23)

Figure 13 shows the effect of uniform temperature change on the load-deformation relationship for the following three cases.

Case A Live load only

Case B Live load + temperature drop = -20°C.

Case C Live load + temperature rise = +20°C.

It is noticeable from fig. 13 that the uniform temperature drop of case B increases the maximum load carried by the double layer grid with percentage of 10% and vice versa for case C.

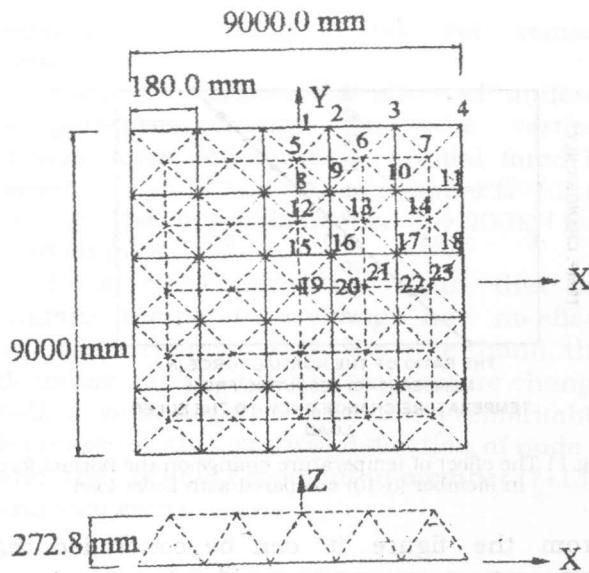


Fig. 12 Model geometry and node numbers of the double layer grid.

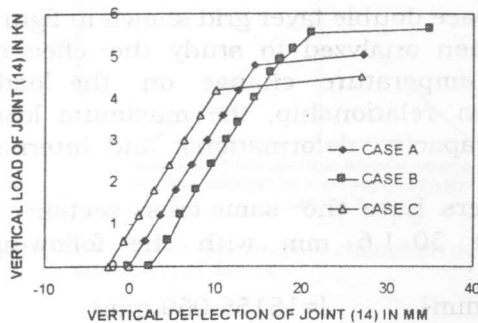


Fig. 13. The effect of temperature changes on the load-deformation relationship.

Figure 14 shows the effect of uniform temperature change on the vertical deflection of node (13), normal force in member (7-14) and M_y of member (7-14) at end 7 relative to that produced by 1 kN concentrated live loads on joints (5,6,7,12,13,14,19,21 and 23), respectively.

From fig. 14 one may recognize that the temperature change has a minor effect on the normal force in member (7-14). Besides, the temperature change has a considerable effect on the deflection of joint (13). Although the effect of temperature change on the bending moment is considerable, it can be neglected because the bending

moment produced in such structures is very small.

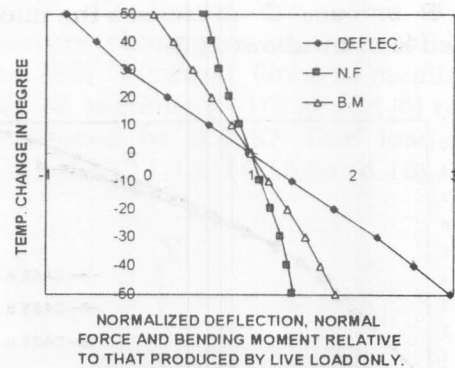


Fig. 14. The effect of temperature change on the deflection and internal forces

Figure 15 shows the normal force in member (7-14) & (11-18) resulting from temperature change only compared with Euler load.

From fig. 15. it can be noticed that the temperature change has an effect on the normal force in member (7-14), e.g. 50°C can produce one fourth of Euler load. Also, it can be concluded that the normal force in members between supports resulting from uniform temperature change is an enormous force and it must be considered in the design of such members.

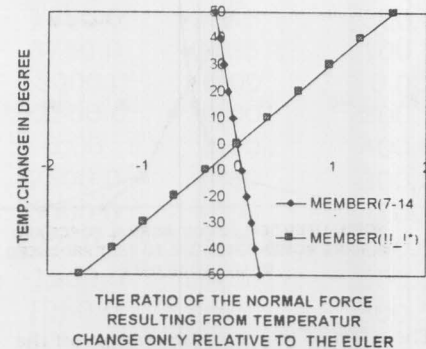


FIG. 15 . The effect of temperature change on the normal force in member (14-21) compared with Euler load

8. Conclusions

The conclusions may be summarized as follows:

- 1-The temperature changes have considerable effect on the behavior of some space structures.
- 2- It is possible for some space frames to be subjected to temperature change and yet the maximum load capacity remains unaltered.
- 3-The maximum load of space domes is seriously affected by the temperature changes than other space frames.
- 4-The maximum load of space double layer grid is considerably affected by temperature changes.
- 5-The temperature changes have considerable effect on deformation of all type of space structures.
- 6- For space single layer domes the effect of temperature changes on the normal force is so destructive that it may produce a normal force in some member equal to or greater than Euler load.
- 7- Excessive temperature drop may cause yielding of some members in single layer domes.
- 8- The shallower the single layer dome the more dangerous the effect of temperature changes.
- 9- The larger the span of the double layer grids the greater the effect of the temperature change on these structures.
- 10- Using moving supports for space structures make them more durable to the temperature changes.
- 11- When using hinged or fixed supports for double layer grids or space trusses, the design forces in members between supports can be approximately calculated as follows

$$P_T = P_{LL} + \alpha \cdot E \cdot A \cdot T_{max} \text{ where}$$

- P_T The total designed force in member.
 P_{LL} The force in member due to live load
 T_{max} The maximum expected temperature change

Notations

The following symbols are used in this paper
 A = cross-section area
 $[B]$ = a local static matrix which relates the relative end displacements of a member in current local x^c, y^c, z^c coordinates to

- the end deformations of the member in the updated local x, y, z coordinates
 $[B]$ = the instantaneous global equilibrium matrix
 b = the width of the cross section in MM
 b_{1n}, b_{2n} = the bowing functions for the base member about axes n (n refers to axes y^c, z^c)
 c_{1n}, c_{2n} = the stability functions of the base member about axes n (n refers to axes y^c, z^c)
 d = the depth of the cross section of a member in MM
 E = modulus of elasticity
 e = change in bar length
 $\{F\}$ = vector of 12×1 represents the element end forces in the direction of its local updated coordinates x, y, z
 G = shear modulus
 $[K_T]$ = a $n \times w$ structure or global tangent stiffness matrix of the whole structure in axes X, Y, Z
 $[k_t]$ = a 12×12 member tangent stiffness matrix in the structure global axes X, Y, Z
 L = initial member length
 L_c = current deformed member length
 $\{P_{ref}\}$ = vector $n \times 1$ represents the reference applied live load in the direction of the global structure coordinates X, Y, Z
 $\{P\}$ = vector $n \times 1$ represents the total applied load = $\sum \{P_{ref}\}$
 $[R]$ = a 12×12 element rotation matrix which relates the element end forces or deformation in the direction of the structure global axes X, Y, Z to their corresponding values in the directions of the element updated local coordinates x, y, z
 $[r]$ = a 3×3 element rotation matrix
 $[t]$ = a 6×6 member tangent stiffness matrix in its local current member coordinates x^c, y^c, z^c
 $[T]$ = a 12×12 member tangent stiffness matrix in the member local axes x, y, z
 T_o = initial temperature
 T = final temperature
 α = coefficient of linear thermal expansion
 $\{v^c\}$ = a vector $n \times 1$ represents the generalized displacements in the directions of the element s current local coordinates x^c, y^c, z^c

{v} = a vector of $n \times 1$ represents the generalized displacements of the structure nodes in the directions of the structure global coordinates X,Y,Z

$\theta_x, \theta_y, \theta_z$ = rotation of node about the global structure X,Y,Z axes

λ^L = live load parameter

References

- [1] H. G. Allen. P. S., and Bulson, "Background to Buckling", McGraw-Hill Book Company, U.K., (1980)
- [2] P. G. Bergan, "Solution algorithm for nonlinear structural problems", Computers and Structures ,Div., Vol. PP.497-509.(1980).
- [3] R. Chandra, D.N. and Trikha, "Nonlinear analysis of steel space structures" J.Struct. Div., ASCE, Vol. 116, No. ST4, April, pp. 898-909 (1990)
- [4] D. J. Dawe, "Matrix and finite element displacement analysis of structures" Department of civil engineering , University of Birmingham
- [5] F. A. Fathelbab, The effect of joints on the stability of shallow single layer lattice dome Ph. D. Thesis , Univ. of Cambridge, (1987)
- [6] K. Fisman, L. Woo, and Namyat, S., "Space frame analysis by matrices and computer" J Struct. Div., ASCE , Vol. 88, No.ST6, December, pp. 245-277 (1962)
- [7] A. Kassimalia, R. and Abbasnia, "Large deformation analysis by matrices and computer" J. Struct. Div., ASCE, Vol. 117, No.ST7, July, pp.2069-2087 (1991)
- [8] H. Klimke, J. and Posch," A modified fictitious force method for the ultimate load analysis of space trusses" Third Int . conference on space structures, 11-14 Sept. PP. 589-593
- [9] C. Oran, "Tangent stiffness in space frames" J. Struct. Div., ASCE, June, PP. 987-1001 (1973)
- [10] J. D. Renton," Stability of space frames by computer analysis" J. Struct. Div., ASCE, Vol.88,No. ST4, August, PP.81-103. (1962)
- [11] S. S. Tezcan, "Computer analysis of plane and space structures," J. Struct. Div., ASCE, Vol. 92, ST2, Apr., PP.143-173. (1966)

Received October 20, 1999
Accepted January 27, 2000